



United States Department of the Interior

U. S. GEOLOGICAL SURVEY

160 N. Stephanie Street
Henderson, NV 89074
Phone: 702-564-4652

September 30, 2014

MEMORANDUM

To: Devin Galloway, WSFT-West Groundwater Specialist, Sacramento, CA
From: Tracie Jackson, Keith Halford, and Amanda Garcia, Hydrologists, Nevada Water Science Center; Don Sweetkind, Geologist, Geologic Division, Denver, CO
Subject: AQUIFER-TEST PACKAGE—Simultaneous numerical analysis of sixteen aquifer tests to estimate hydraulic properties on Pahute Mesa, Nevada National Security Site

This memorandum documents the simultaneous interpretation of 16 multiple-well aquifer tests to estimate hydraulic properties on Pahute Mesa, Nevada National Security Site (NNSS). Multiple-well aquifer tests were conducted by Navarro-Intera, LLC (N-I) between November 2009 and May 2014 ([Table 1](#)). A cumulative volume of 63 million gallons was pumped during these aquifer tests so that drawdowns could be observed in a network of 34 wells. Water levels in these observation wells have been measured continuously by N-I and the U.S. Geological Survey (USGS). The primary purpose of this analysis is to estimate total transmissivity around each pumping well. Estimates of transmissivity and storage properties for the volcanic rocks at Pahute Mesa are needed to constrain hydraulic properties in groundwater flow and contaminant transport models at the NNSS. This work expands on a previous investigation where 8 of the 16 multiple-well aquifer tests were interpreted simultaneously (Halford, Fenelon, and Reiner, 2012).

The 16 multiple-well aquifer tests used pumping wells that contained a main casing with either single or multiple completions. In pumping wells with multiple completions in the main casing, packers were used to separate completions so that distinct intervals could be pumped as individual aquifer tests. Aquifer tests in multiple completion wells are reported herein with the designation of main upper zone, main intermediate zone, or main lower zone. Many pumping wells also contained piezometers completed in the annulus alongside the main completion zone or in shallower or deeper zones within the borehole. Piezometers in wells with multiple completions are reported herein as observation wells with the designation of shallow, intermediate, or deep. During an aquifer test, water levels in the pumping well and in a network of observation wells were monitored with pressure transducers ([Figure 1](#); [Appendix A](#)). Distances between pumping and observation wells range from less than one foot to a few miles.

Table 1. Pumping periods and volumes pumped during each aquifer test.

Pumping Well	Period of Analysis		Volume pumped, in millions of gallons	Reference
	Begin	End		
<i>ER-20-4 main</i>	08/30/2011	09/21/2011	5.2	Mirus and others, 2012a
<i>ER-20-7</i>	09/14/2010	09/24/2010	2.4	Halford and others, 2011
<i>ER-20-8 main upper zone</i>	05/18/2011	06/27/2011	3.1	Garcia and others, 2012; Halford and others, 2011
<i>ER-20-8 main lower zone</i>	07/15/2011	08/08/2011	3.1	Garcia and others, 2012
<i>ER-20-8 #2 main</i>	11/28/2009	12/18/2009	1.9	Halford, Fenelon, and Reiner, 2010
<i>ER-20-11</i>	06/11/2013	08/05/2013	10.8	Jackson and others, 2014
<i>ER-EC-11 main</i>	04/30/2010	05/19/2010	5.5	Halford, Fenelon, and Reiner, 2010
<i>ER-EC-12 main upper zone</i>	10/11/2011	11/28/2011	2.6	Mirus and others, 2012b
<i>ER-EC-12 main lower zone</i>	02/29/2012	03/19/2012	<0.1	Mirus and others, 2012b
<i>ER-EC-13 main upper zone</i>	06/22/2012	08/02/2012	8	Damar and others, 2013a
<i>ER-EC-13 main lower zone</i>	03/07/2013	03/29/2013	5.8	Damar and others, 2013b
<i>ER-EC-14 main upper zone</i>	03/14/2014	04/07/2014	4	Garcia and others, 2014
<i>ER-EC-14 main lower zone</i>	04/18/2014	05/12/2014	7	Garcia and others, 2014
<i>ER-EC-15 main upper zone</i>	09/17/2013	10/29/2013	2.9	Halford and Reiner, 2014
<i>ER-EC-15 main intermediate zone</i>	12/18/2013	01/10/2014	<0.1	Halford and Reiner, 2014
<i>ER-EC-15 main lower zone</i>	01/22/2014	02/18/2014	0.5	Halford and Reiner, 2014

Drawdowns from pumping wells were used to obtain hydraulic property estimates across a well network comprising pumping, observation, and background wells (Figure 1; Table 2). Drawdowns were estimated from measured water levels because water-level measurements are affected by environmental water-level fluctuations in addition to pumping signals (Garcia and others, 2013). Drawdown estimates were differentiated from environmental fluctuations with analytical water-level models (Halford, Garcia, and Reiner, 2012). Drawdowns from aquifer tests at well sites *ER-20-11*, *ER-EC-14*, and *ER-EC-15* were estimated during 2014 (Garcia and others, 2014; Jackson and Halford, 2014). More than 200 drawdown time series were estimated for pumping and observation well pairs that are separated by horizontal distances between 0 and 23,000 ft. These drawdown estimates were documented previously in nine supporting memoranda (See **Appendix D**) (Table 1). Well construction (Table 2), water-level collection, and discharge measurements also were documented in these supporting memoranda.

Hydraulic properties were estimated with numerical groundwater flow models by fitting simulated drawdowns to drawdowns estimated from measured water levels. Separate numerical models characterizing the 16 multiple-well aquifer tests were created and analyzed simultaneously because of the effects of drawdown interference in aquifers affected by multiple aquifer tests. Simultaneous interpretation of all tests assured that a consistent set of hydraulic properties were being estimated. Generally, for multiple completion pumping wells, aquifer tests from different open intervals were analyzed with a single model because the second test typically occurred within a month of the first test and water levels in distant observation wells simultaneously were affected by both aquifer tests. Site *ER-EC-13* was an exception because the system recovered during the 7 months between the end of the *ER-EC-13 main upper zone* aquifer test and *ER-EC-13 main lower zone* aquifer test. In total, 11 numerical models were created to simulate drawdowns from the 16 aquifer tests.

A typical “aquifer test”, as simulated in the numerical model, consisted of about 10 days of intermittent pumping to develop the well and perform step-drawdown tests, followed by about 10 days of continuous pumping at a constant-rate. Pumping periods were shorter in low-productivity wells where pumping could not be sustained (*ER-EC-12 main lower zone*, and *ER-EC-15 main intermediate and lower zones*) or in contaminated wells with limited capacity for storage of discharge water (*ER-20-7*). Pumping periods and total volumes pumped for each of the aquifer tests are summarized in [Table 1](#).

Table 2. Well location and construction data for analyzed wells during multiple-well aquifer testing at Pahute Mesa, Nevada National Security Site.

[Latitude and longitude are in degrees, minutes, and seconds and referenced to North American Datum of 1927 (NAD27); ft amsl, feet above National Geodetic Vertical Datum of 1988 (NGVD29); ft bgs, feet below ground surface.]

Map Identifier	Site Identifier	Latitude	Longitude	Ground surface elevation, ft amsl	Depth to Static Water Level, ft bgs	Diameter Screen, in inches	Top Screen, ft bgs	Bottom Screen, ft bgs
Pumping Wells								
<i>ER-20-4 main</i>	371143116262503	N37°11'43"	W116°26'25"	5,736	1,521	6 5/8	2,479	3,002
<i>ER-20-7</i>	371247116284502	N37°12'47"	W116°28'45"	6,209	2,023	5 1/2	2,360	2,875
<i>ER-20-8 main upper zone</i>	371135116282601	N37°11'35"	W116°28'26"	5,848	1,667	5 1/2	2,471	2,940
<i>ER-20-8 main lower zone</i>	371135116282601	N37°11'35"	W116°28'26"	5,848	1,667	5 1/2	3,095	3,440
<i>ER-20-8 #2 main</i>	371135116282701	N37°11'35"	W116°28'27"	5,849	1,668	7 5/8	1,680	2,263
<i>ER-20-11</i>	371146116290301	N37°11'46"	W116°29'03"	5,834	1,655	6 5/8	2,609	2,963
<i>ER-EC-11 main</i>	371151116294101	N37°11'51"	W116°29'41"	5,656	1,476	7 5/8	3,134	3,385
<i>ER-EC-12 main upper zone</i>	371024116293101	N37°10'24"	W116°26'25"	5,532	1,364	6 5/8	1,893	2,744
<i>ER-EC-12 main lower zone</i>	371024116293101	N37°10'24"	W116°29'31"	5,532	1,364	6 5/8	3,231	3,770
<i>ER-EC-13 main upper zone</i>	371010116325401	N37°10'10"	W116°32'54"	5,175	1,012	6 5/8	1,888	2,097
<i>ER-EC-13 main lower zone</i>	371010116325401	N37°10'10"	W116°32'54"	5,175	1,012	6 5/8	2,286	2,601
<i>ER-EC-14 main upper zone</i>	370825116302401	N37°08'25"	W116°30'41"	5,186	1,023	6 5/8	1,359	1,666
<i>ER-EC-14 main lower zone</i>	370825116302401	N37°08'25"	W116°30'41"	5,186	1,023	6 5/8	1,953	2,264
<i>ER-EC-15 main upper zone</i>	371110116310501	N37°11'10"	W116°31'05"	5,365	1,191	7 5/8	1,393	1,739
<i>ER-EC-15 main intermediate zone</i>	371010116325401	N37°11'10"	W116°31'05"	5,365	1,191	5 1/2	2,157	2,408
<i>ER-EC-15 main lower zone</i>	371010116325401	N37°11'10"	W116°31'05"	5,365	1,191	5 1/2	2,807	3,122

Table 2—Continued.

Map Identifier	Site Identifier	Latitude	Longitude	Ground surface elevation, ft amsl	Depth to Static Water Level, ft bgs	Diameter Screen, in inches	Top Screen, ft bgs	Bottom Screen, ft bgs
Observation Wells								
ER-20-1	371321116292301	N37°13'21"	W116°29'29"	6,181	1,989	24	N/A	N/A
ER-20-2-1	371246116240101	N37°12'46"	W116°24'01"	6,705	2,274	2 7/8	2,368	2,494
ER-20-4 deep	371143116262503	N37°11'43"	W116°26'25"	5,736	1,521	2 7/8	2,485	3,002
ER-20-4 shallow (main)	371143116262504	N37°11'43"	W116°26'25"	5,736	1,521	2 7/8	1,521	1,602
ER-20-5-1	371312116283801	N37°13'12"	W116°28'38"	6,242	2,053	2 7/8	2,315	2,374
ER-20-5-3	371311116283801	N37°13'11"	W116°28'38"	6,242	2,057	2 7/8	3,430	3,882
ER-20-7	371247116284502	N37°12'47"	W116°28'45"	6,209	2,023	5 1/2	2,360	2,875
ER-20-8 deep	371135116282602	N37°11'35"	W116°28'26"	5,848	1,667	1 3/50	3,141	3,302
ER-20-8 intermediate	371135116282604	N37°11'35"	W116°28'26"	5,848	1,667	2 19/50	2,498	2,909
ER-20-8 shallow	371135116282701	N37°11'35"	W116°28'26"	5,848	1,667	2 19/50	1,680	2,263
ER-20-8 #2	371135116282701	N37°11'35"	W116°28'27"	5,849	1,668	2 19/50	1,680	2,263
ER-20-11	371146116290301	N37°11'46"	W116°29'03"	5,834	1,655	2 19/50	2,609	2,963
ER-EC-1	371223116314701	N37°12'23"	W116°31'47"	6,026	1,856	5 1/2	2298 3348 4488	2821 3760 4750
ER-EC-2A	370852116340502	N37°08'42"	W116°34'03"	4,902	755	5 1/2	1707 3077 4487	2179 3549 4916
ER-EC-6 deep	371120116294803	N37°11'20"	W116°29'48"	5,604	1,426	2 19/50	3437 4420	3811 4904
ER-EC-6 intermediate	371120116294804	N37°11'20"	W116°29'48"	5,604	1,425	1 9/10	2,194	2,507
ER-EC-6 shallow	371120116294805	N37°11'20"	W116°29'48"	5,604	1,425	2 19/50	1,628	1,870
ER-EC-11 deep	371151116294102	N37°11'51"	W116°29'41"	5,656	1,476	2 7/8	3,641	4,094
ER-EC-11 intermediate	371151116294103	N37°11'51"	W116°29'41"	5,656	1,476	2 19/50	3,159	3,378
ER-EC-11 shallow	371151116294104	N37°11'51"	W116°29'41"	5,656	1,476	2 19/50	2,678	2,991
ER-EC-12 deep	371024116293102	N37°10'24"	W116°26'25"	5,532	1,364	2	3,877	3,919
ER-EC-12 intermediate	371024116293103	N37°10'24"	W116°26'25"	5,532	1,364	2	3,240	3,722
ER-EC-12 shallow	371024116293104	N37°10'24"	W116°26'25"	5,532	1,364	2	1,919	2,681
ER-EC-13 deep	371010116325402	N37°10'10"	W116°32'54"	5,175	1,012	2 7/8	2,292	2,611
ER-EC-13 intermediate	371010116325403	N37°10'10"	W116°32'54"	5,175	1,012	2 7/8	1,900	2,100
ER-EC-13 shallow	371010116325404	N37°10'10"	W116°32'54"	5,175	1,012	2 7/8	1,014	1,094
ER-EC-14 deep	370825116302402	N37°08'25"	W116°30'41"	5,186	1,023	2 7/8	1,945	2,257
ER-EC-14 shallow	370825116303403	N37°08'25"	W116°30'41"	5,186	1,023	2 7/8	1,352	1,664
ER-EC-15 deep	371110116310502	N37°11'10"	W116°31'05"	5,365	1,191	2 7/8	2,800	3,120
ER-EC-15 intermediate	371110116310503	N37°11'10"	W116°31'05"	5,365	1,191	2 7/8	2,156	2,395
ER-EC-15 shallow	371110116310504	N37°11'10"	W116°31'05"	5,365	1,191	2 7/8	1,381	1,741
UE-18r	370806116264001	N37°08'15"	W116°26'41"	5,538	1,363	10 1/20	1,381	1,741

Table 2—Continued.

Map Identifier	Site Identifier	Latitude	Longitude	Ground surface elevation, ft amsl	Depth to Static Water Level, ft bgs	Diameter Screen, in inches	Top Screen, ft bgs	Bottom Screen, ft bgs
Background Wells								
ER-18-2	370615116222401	N37°06'14"	W116°22'22"	5,437	1,210	5 1/2	1,351	2,500
ER-20-6-3	371533116251801	N37°15'33"	W116°25'18"	6,466	2,014	2 7/8	2,436	2,807
ER-EC-4	370935116375301	N37°09'32"	W116°37'52"	4,760	748	5 1/2	952	2,295
ER-EC-5	370504116335201	N37°05'04"	W116°33'52"	5,077	1,016	5 1/2	1,169	2,500
ER-EC-7	365910116284401	N36°59'06"	W116°28'40"	4,805	746	5 1/2	895	1,386
ER-EC-8	370610116345301	N37°06'10"	W116°37'53"	4,334	323	5 1/2	683 1447 1676	984 1507 1908
PM-1	371649116242101	N37°16'49"	W116°24'21"	6,558	2,099	9 19/25	7,543	7,858
PM-3-1	371421116333703	N37°14'21"	W116°33'37"	5,823	1,457	2 7/8	1,919	2,144
U-20WW	371505116254501	N37°15'05"	W116°25'45"	6,468	2,053	17 1/2	2,864	3,268
U-20a-2WW	371434116251601	N37°43'41"	W116°25'16"	6,472	2,089	10 5/8	860	4,500
U-20bg	371414116242901	N37°14'14"	W116°24'29"	6,567	2,137	96	540	2,200
UE-18r	370806116264001	N37°08'06"	W116°26'40"	5,538	1,363	10 1/20	1,629	5,004
UE-18t	370741116194501	N37°07'41"	W116°19'45"	4,288	913	2 19/50	1,896	2,600
UE-19b-1	371852116175701	N37°18'52"	W116°17'57"	6,802	2,117	13 17/50	2,190	4,500
UE-19c	371608116191002	N37°16'08"	W116°19'10"	7,033	2,339	1 3/5	2,421	8,489
UE-19e	371750116195901	N37°17'50"	W116°19'59"	6,919	2,220	13 17/50	2,475	6,005
UE-19fS	371329116220302	N37°13'29"	W116°22'03"	6,735	2,337	9 7/8	2,565	4,779
UE-19gS	371830116215300	N37°18'30"	W116°21'53"	6,719	2,033	8 31/50	2,650	7,500
UE-19h	372034116222501	N37°20'34"	W116°22'25"	6,780	2,111	2 7/8	2,287	2,321
UE-19i	371459116204812	N37°14'59"	W116°20'48"	6,839	2,374	9 7/8	2,896	8,000
UE-20bh 1	371442116243301	N37°14'42"	W116°24'33"	6,637	2,213	12 31/50	1,941	2,810
UE-20d	371452116284901	N37°14'52"	W116°28'49"	6,253	2,075	12 31/50	2,075	4,075
UE-20e-1	371901116272501	N37°19'01"	W116°27'25"	6,297	1,822	12 31/50	1,820	3,820
UE-20f	371617116291701	N37°16'17"	W116°29'17"	6,116	1,879	6 1/8	4,556	13,686
UE-20h	371618116260201	N37°16'18"	W116°26'02"	6,557	2,165	12 31/50	2,518	7,207
UE-20j	371801116320301	N37°18'01"	W116°32'03"	5,903	1,270	12 31/50	1,740	5,690
UE-20n 1	371425116251902	N37°14'25"	W116°25'19"	6,461	2,041	8 23/25	2,308	2,834
WW-8	370956116172101	N37°09'56"	W116°17'21"	5595	1080	7 1/50	30	2031

Hydrogeology

The wells monitored during multiple-well aquifer testing at Pahute Mesa are completed in Tertiary volcanic rocks. The volcanic rocks of Pahute Mesa are dominated by lavas and tuffs of rhyolitic composition (Laczniak and others, 1996). Geologic structures at Pahute Mesa include normal faults, some with surface exposure, and buried structural zones and caldera margins (Figure 1).

Structural features offset the hydrostratigraphy encountered in wells at Pahute Mesa. The Northern Timber Mountain Moat Structural Zone (NTMMSZ) is a buried west-northwest trending fault zone (Figure 1) that displaces rocks by more than 1,000 ft (U.S. Department of Energy, 2010a). The area that is bounded on the north by the NTMMSZ and on the south by the Timber Mountain caldera complex structural margin is referred to as “the Bench” (U.S. Department of Energy, 2009). South of the Bench is the Timber Mountain moat structural domain, a structural region that is the northwestern moat area of the Timber Mountain caldera complex (U.S. Department of Energy, 2011a).

Observation wells north of the Bench and west of the Boxcar fault (Figure 1) penetrate about 2,000 ft of unsaturated rock. Major water-producing hydrostratigraphic units (HSUs) are the Tiva Canyon aquifer (TCA) and Topopah Spring aquifer (TSA), with some production from lava-flow aquifers in the Calico Hills zeolitic composite unit (CHZCM) (Appendix A). North of the Bench and east of the Boxcar fault, well *ER-20-4* penetrates about 1,500 ft of unsaturated rock and produces water from a lava-flow aquifer within the CHZCM.

Observation wells in the Bench (Figure 1) penetrate about 1,200 to 1,800 ft of unsaturated rock. Wells in the Bench were constructed to monitor five water-producing HSUs: the upper Paintbrush lava-flow aquifer (UPLFA), Benham aquifer (BA), Scrugham Peak aquifer (SPA), TCA, and TSA. The CHZCM and Crater Flat composite unit (CFCM) also supply water to observation wells on the Bench (Appendix A).

Observation wells south of the Bench (Figure 1) penetrate about 750 to 1,000 ft of unsaturated rock. The three water-producing HSUs in wells in this area are lava-flow aquifers within the Fortymile Canyon composite unit (FCCM) and welded-tuff aquifers of the Timber Mountain composite unit (TMCM) and Timber Mountain aquifer (TMA).

The lithologies of major water-producing HSUs in the aquifer-test area are rhyolitic lava flows (UPLFA, BA and SPA) and welded ash-flow tuffs (TCA, TSA, and TMA) (U.S. Department of Energy, 2010b and 2011b). The FCCM, CHZCM, and CFCM are composite units of rhyolitic lava-flow aquifers and non-welded tuff confining units with local to common zeolitization (Laczniak and others, 1996, p.11; U.S. Department of Energy, 1997; 2000). The CFCM also contains welded-tuff aquifers. The TMCM in the study area is a composite of welded-tuff aquifers and non-welded tuff confining units (U.S. Department of Energy, 2002a).

Aquifer-Test Analysis

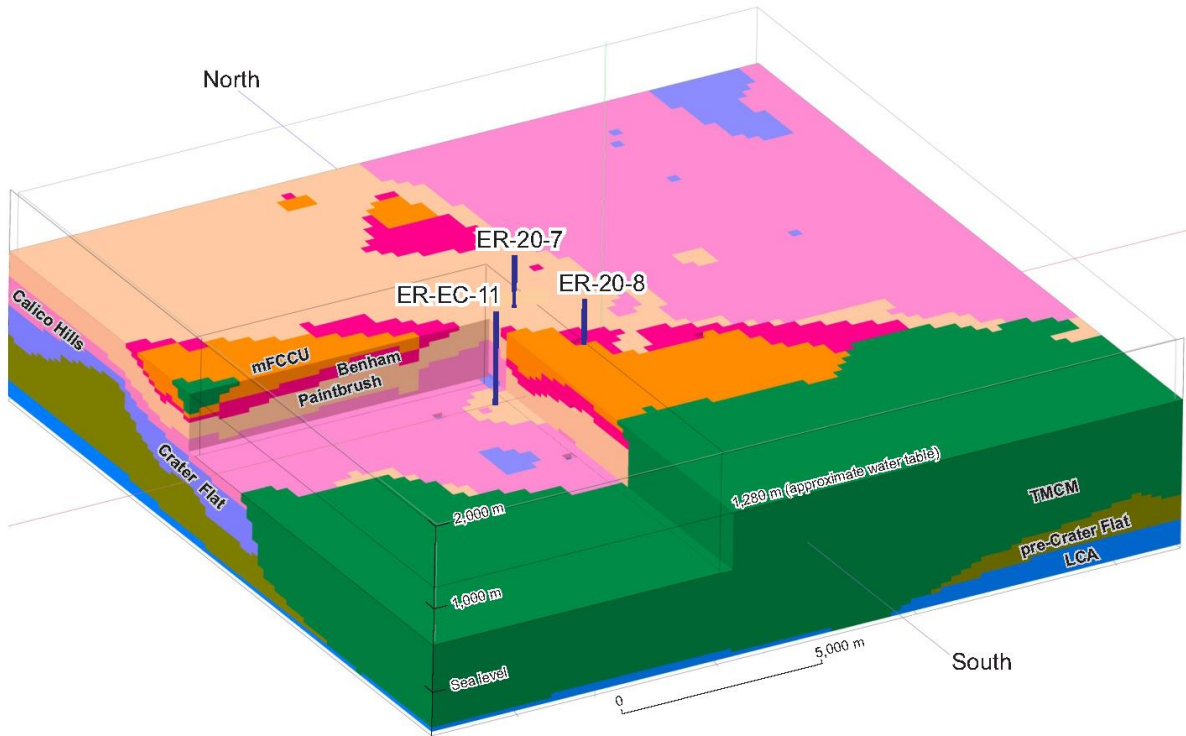
Aquifer-test results were analyzed with numerical models to estimate hydraulic properties for the volcanic rocks underlying Pahute Mesa. Numerical methods were used because the groundwater beneath the study area flows through a complexly layered sequence of volcanic-rock aquifers and confining units that have been faulted into distinct structural blocks. Observation wells are often vertically separated and distant from the pumping wells. Therefore, water-level responses in the observation wells could not be analyzed with simple analytical methods, such as the Theis solution (Theis, 1935), because simplifying assumptions of the methods were violated.

Hydraulic properties of aquifers and confining units were estimated by interpreting drawdowns from multiple aquifer tests using a single, three-dimensional hydrogeologic framework and multiple groundwater-flow models. Multiple groundwater-flow models allowed grid refinement near each pumping well and different pumping schedules specific to each aquifer test. Multiple groundwater-flow models also facilitate independent aquifer test assessments and provide assurance that simulated drawdowns and sensitivities are computed and extracted correctly.

Hydrogeologic Framework Model

A single conceptual model of the hydrogeologic framework was used to interpret aquifer-test results. Many conceptual models exist for distributing hydraulic properties beneath Pahute Mesa, including those where hydraulic properties of mapped faults and structural zones differ from hydraulic properties of the HSUs. Interpretation of hydraulically unique fault structures was beyond the primary scope of estimating total transmissivity around each of the pumped wells. Because fault structures were not differentiated in either the hydrogeologic framework model or in the groundwater flow models, the hydraulic properties of fault structures could not be estimated.

Hydraulic properties were distributed spatially with a single, three-dimensional hydrogeologic framework that was constructed from wellbore data, refined cross-sections using data from newly drilled wells (Sigmund Drellack, National Security Technologies, LLC., written commun., 2011), and HSU picks from the Pahute Mesa Corrective Action Unit (CAU) framework model (Bechtel Nevada, 2002) (Figure 2). The hydrogeologic framework was discretized vertically into 51 layers between 1,700 ft below sea level and 6,500 ft above sea level, where each layer was about 164 ft thick. The hydrogeologic framework for this study used 15 modified HSUs (Table 3). Existing HSUs were modified so that observed hydraulic responses could be adequately replicated with the groundwater-flow models.



Framework model layer	Modified HSU abbreviation	Hydrostratigraphic units
TMCM	TMCM	TMCM
mFCCU	mFCCU	THLFA, THCM, TMA, FCCU, WWA, PVTA
Benham	BA/SPA	BA, SPA
Paintbrush	mUPCU, TCA, LPCU, TSA	UPCU, MPCU, TCA, LPCU, TSA
Calico Hills	mCHZCM	CHVCM, CHZCM, CHCU, IA
Crater Flat	mCFCM	CFCM, CFCU, BFCU
pre-Crater Flat	mCFCM	BRA, PBRCM
LCA	mCFCM	LCA

Figure 2. Three-dimensional, hydrogeologic framework of hydrostratigraphic units for distributing hydraulic properties. The modified Fluorspar Canyon confining units (mFCCU), Paintbrush units, and Timber Mountain composite units (TMCM) were subdivided into six units, four units, and five units, respectively, in the hydrogeologic framework. The mFCCU, Paintbrush units, and TMCM are each shown here as one unit for illustrative purposes. Hydrostratigraphic unit abbreviations are described in [Table 3](#).

Table 3. Existing and modified hydrostratigraphic units.

HSU name	HSU abbreviation	Modified HSU abbreviation
Thirsty Canyon volcanic aquifer	TCVA	Not present
Timber Mountain composite unit, 1	TMCM	TMCM1
Timber Mountain composite unit, 2	TMCM	TMCM2
Timber Mountain composite unit, 3	TMCM	TMCM3
Timber Mountain composite unit, 4	TMCM	TMCM4
Timber Mountain composite unit, 5	TMCM	TMCM5
Tannenbaum Hill lava-flow aquifer	THLFA	mFCCU
Tannenbaum Hill composite unit	THCM	mFCCU
Timber Mountain aquifer	TMA	mFCCU
Fluorspar Canyon confining unit	FCCU ¹	mFCCU
Windy Wash aquifer	WWA	mFCCU
Paintbrush vitric-tuff aquifer	PVTA	mFCCU
Benham aquifer	BA	BA/SPA
Scrugham Peak aquifer	SPA	BA/SPA
Upper Paintbrush confining unit	UPCU	mUPCU
Middle Paintbrush confining unit	MPCU	mUPCU
Tiva Canyon aquifer	TCA	TCA
Lower Paintbrush confining unit	LPCU	LPCU
Topopah Spring aquifer	TSA	TSA
Calico Hills vitric composite unit, Upper	CHVCM	mCHZCMu
Calico Hills vitric composite unit, Lower	CHVCM	mCHZCMI
Calico Hills vitric composite unit	CHVCM	mCHZCM
Calico Hills zeolitic composite unit	CHZCM	mCHZCM
Calico Hills confining unit	CHCU	mCHZCM
Inlet aquifer	IA	mCHZCM
Crater Flat composite unit	CFCM	mCFCM
Crater Flat confining unit	CFCU	mCFCM
Bullfrog confining unit	BFCU	mCFCM
Belted Range aquifer	BRA	mCFCM
Pre-Belted Range composite unit	PBRCM	mCFCM
Lower carbonate aquifer	LCA	mCFCM

¹Comprises majority of the saturated thickness of the mFCCU modified HSU in the vicinity of the aquifer tests

Hydrostratigraphic units in the bench area (Figure 1) were modified by grouping certain HSUs based on either hydraulically similar properties (e.g., BA/SPA) or the presence of multiple thin HSUs where their hydraulic properties cannot be differentiated in the groundwater-flow model (e.g., HSUs in the mCFCM). The THLFA, THCM, TMA, FCCU, WWA, and PVTA were undifferentiated to form one modified HSU, denoted mFCCU, where the FCCU comprises the majority of the saturated thickness (Table 3). The joint Benham and Scrugham Peak aquifers (BA/SPA) modified HSU incorporates the BA and SPA units. A modified Upper Paintbrush confining unit (mUPCU) combined the UPCU and MPCU units. A modified Calico Hills zeolitic composite unit (mCHZCM) aggregated the CHVCM, CHZCM, CHCU, and IA units. A modified Crater Flat composite unit (mCFCM) combined the CFCM, CFCU, BFCU, BRA, PBRCM, and LCA units.

The mCHZCM was differentiated further north of the NTMMSZ because of observed drawdowns in well *ER-20-4 shallow* during the *ER-20-4 main* aquifer test (Halford, Garcia, and Reiner, 2012). The mCHZCM was divided into two HSUs at an altitude of about 3,600 ft so that hydraulic conductivity could differ vertically between wells *ER-20-4 shallow* and *ER-20-4 main*. The modified upper and lower HSUs were mCHZCMu and mCHZCMI, respectively. Hydraulic conductivity of mCHZCMu was expected to be less than the hydraulic conductivity of the mCHZCMI because the upper HSU primarily is bedded tuff near site *ER-20-4*, whereas the mCHZCMI is stony rhyolite lava. The mCHZCMu laterally extends east of the West Boxcar fault and north of the NTMMSZ (Figure 1).

The TMCM was differentiated into 5 HSUs south of the Bench area based on observed drawdowns during aquifer tests at the *ER-EC-13* site (Halford and Reiner, 2013). The TMCM was differentiated into two lava-flow aquifers that intersect the upper and lower screens in wells *ER-EC-13 main* and *ER-EC-14 main*. These two lava-flow aquifers are overlain, separated, and underlain by ash-flow tuff confining units (U.S. Department of Energy, 2011a). The ash-flow tuffs adjacent to the lava-flow aquifers are non-welded and zeolitized, and similar units at Pahute Mesa typically are characterized as confining units (Laczniaik and others, 1996, p.11; U.S. Department of Energy, 1997).

Hydrostratigraphic unit displacements along the NTMMSZ, Timber Mountain caldera complex structural margin, Thirsty Canyon lineament, ER-20-7 fault, ER-20-8 fault, West Boxcar fault, and West Greeley fault were simulated (Figure 1). Displacements along all other fault structures were considered minor and were not simulated explicitly.

Estimating Hydraulic Properties with Pilot Points

Hydraulic conductivity was distributed throughout each of the modified HSUs with pilot points. Pilot points are locations in the model domain where hydraulic properties are estimated (RamaRao and others, 1995). Pilot points were assigned to modified HSUs at 182 mapped locations (Figure 3), with a denser spacing of pilot points specified around the pumped wells (Figures 3 and 4). Modified HSUs were spatially discontinuous in the model domain, causing modified HSU extents to be locally absent within parts of the mapped pilot point area. Therefore, less than 182 pilot points existed in any modified HSU because pilot points were not defined in locations where an HSU was absent. For example, the TMCM only is present south of the Timber Mountain caldera complex structural margin (Figures 2 and 3); therefore, for the TMCM, pilot points were not defined north of the Timber Mountain caldera complex structural margin where the TMCM does not exist in the model domain. Hydraulic conductivity was distributed with a total of 996 pilot points across all HSUs. Local hydraulic conductivity extremes were minimized by assigning homogeneous hydraulic conductivities around pumping and observation wells (tied pilot points on Figures 3 and 4). Homogeneous conditions around a well were defined by a ring of pilot points that were assigned a single, estimable hydraulic conductivity (Figure 4). This reduced the number of estimable pilot points by 251.

Hydraulic conductivities at background wells were assigned from previous aquifer-test results (Table 4) to bound hydraulic property estimates outside the area of investigation because hydraulic property estimates are insensitive to measurement observations. The area of investigation is defined where maximum drawdown was greater than or equal to 0.05 ft during simulation of any aquifer test (see section “Area Investigated” for details), and occurs within an 80 mi² area shown in Figure 4. The numerical model domain for each aquifer test is about 5,400 mi², and includes the area shown in Figure 3; the west and east model domain boundaries extend beyond the edge of Figure 3 by about 4 mi.

Hydraulic conductivity estimates at background wells that were assigned to HSUs at background well locations were interpreted from transmissivity estimates and flow logs in a previous investigation (Garcia and others, 2010). Assigned transmissivities at background wells in NNSS areas 19 and 20 bound hydraulic property estimates in the northern and eastern extents of the model domain (Figure 3). Assigned transmissivities at background wells in NNSS area 18 and south of the Timber Mountain caldera complex structural margin bound hydraulic property estimates in the southern and western extents of the model domain. About 60 percent of the hydraulic conductivity values were estimated after assigning values at previous aquifer-test sites and defining rings of homogeneous hydraulic conductivities around pumping and observation wells (Figure 3).

Assigned pilot points also were used to distribute specific yield and specific storage (Figure 3). Specific yield was distributed with 126 adjustable pilot points at the water table. Specific storage was distributed with 646 adjustable pilot points. Specific yield of fractured rocks was expected to range between 0.001 and 0.05. Specific storage initially was assigned as 1.5×10^{-6} 1/ft and was allowed to range between 1×10^{-8} and 4×10^{-5} 1/ft. The range of estimated specific storages is greater than the expected range (U.S. Geological Survey, 2014). This large range was permitted to compensate for potential errors in the framework model. For example, a specific storage estimate of 1×10^{-7} 1/ft can be reasonable if the simulated feature is 5,000 ft thick and the actual transmissive feature is 400 ft thick. Vertical-to-horizontal anisotropy was assumed equal to 1 and was not estimated.

Hydraulic properties were laterally interpolated between pilot points with kriging to node locations defined within each groundwater-flow model (Doherty, 2008b). The spatial variability of log-hydraulic conductivity was defined with an isotropic, exponential variogram, where the specified range was 15,000 ft (a nugget was not specified). Hydraulic properties within an HSU were assumed vertically constant. Therefore, laterally interpolated hydraulic properties from each HSU were assigned to all layers within the HSU in the groundwater-flow model (Figure 5).

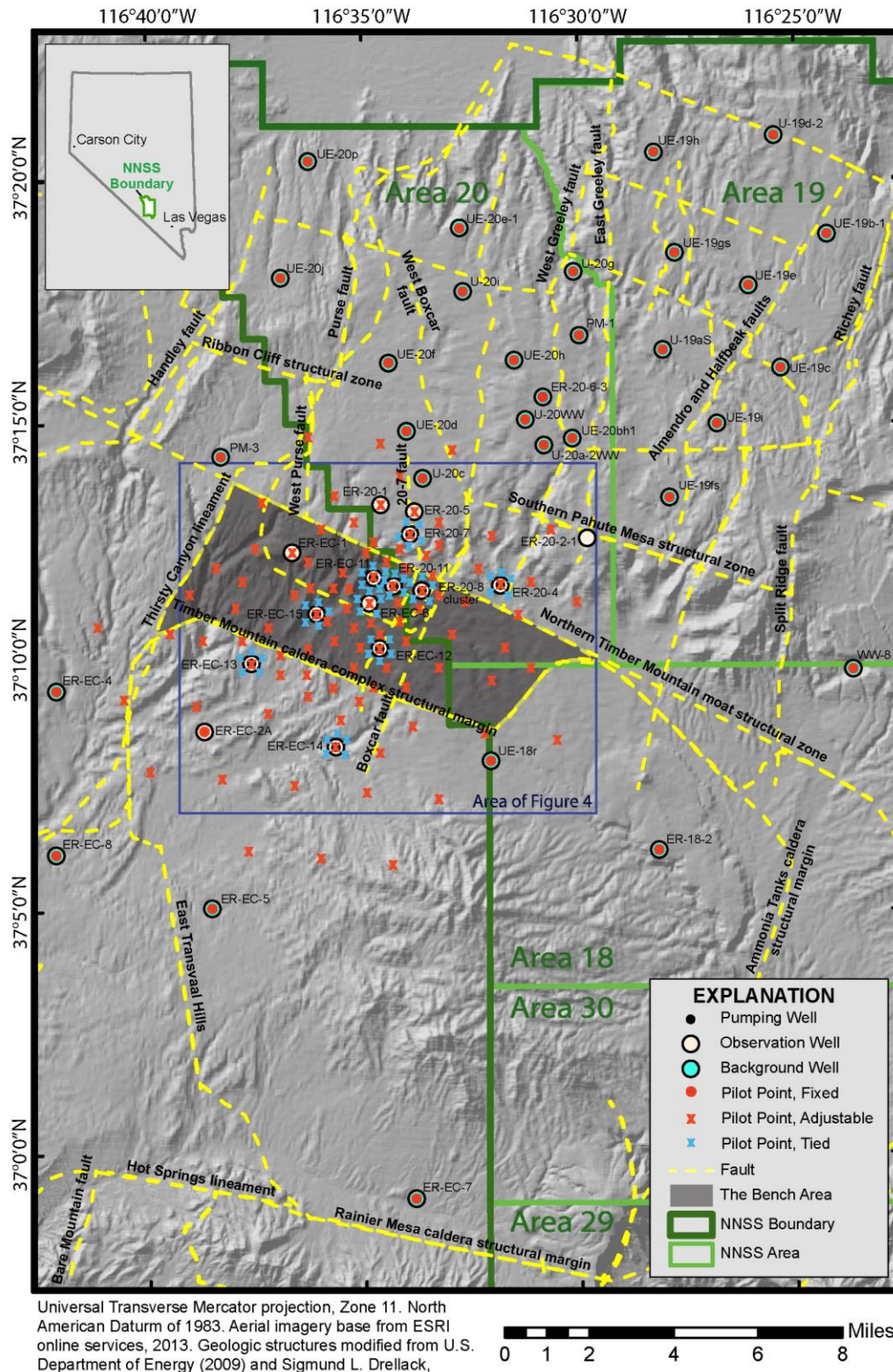
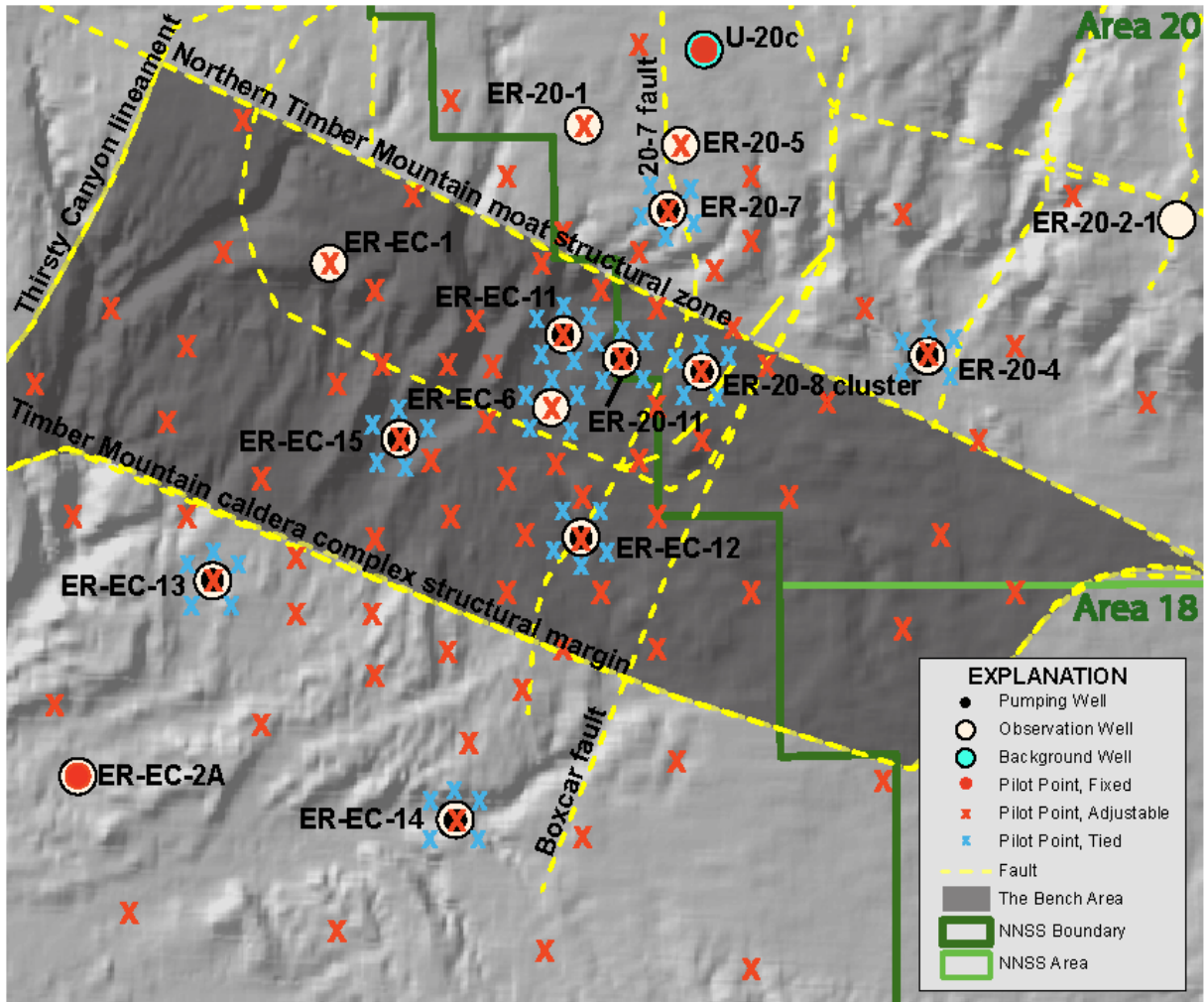


Figure 3. Locations of pilot points simulated in numerical models for each of the 16 multiple-well aquifer tests.



Universal Transverse Mercator projection, Zone 11. North American Datum of 1983. Aerial imagery base from ESRI online services, 2013. Geologic structures modified from U.S. Department of Energy (2009) and Sigmund L. Drellack, National Security Technologies, LLC, written commun. (2011).

0 1 2 Miles

Figure 4. Locations of pilot points near pumped and monitored observation wells that were simulated in numerical models for each of the 16 multiple-well aquifer tests.

Table 4. Transmissivity estimates from previous aquifer tests.

USGS Site Identification Number	Pumping Well Name	Reference	Transmissivity, in feet squared per day
370615116222401	<i>ER-18-2</i>	U.S. Department of Energy, 2002b	2
371321116292301	<i>ER-20-1</i>	Halford, Fenelon, and Reiner, 2012	5,300
371312116283801	<i>ER-20-5</i>	U.S. Department of Energy, 1997	3,100
371533116251801	<i>ER-20-6-3</i>	Garcia and others, 2010	3,600
371223116314701	<i>ER-EC- 1</i>	Garcia and others, 2010	7,000
370852116340501	<i>ER-EC- 2A</i>	Oberlander, 2002	200
370935116375301	<i>ER-EC- 4</i>	Garcia and others, 2010	50,000
370504116335201	<i>ER-EC- 5</i>	Oberlander, 2002	14,000
371120116294801	<i>ER-EC- 6</i>	Garcia and others, 2010	270
365910116284401	<i>ER-EC- 7</i>	Oberlander, 2007	10,000
370610116375301	<i>ER-EC- 8</i>	U.S. Department of Energy, 2002c	3,700
371649116242101	<i>PM-1</i>	Belcher and Elliott, 2001	2
371421116333702	<i>PM-3</i>	Belcher and Elliott, 2001	50
371630116221201	<i>U-19aS</i>	Belcher and Elliott, 2001	2
372054116191901	<i>U-19d-2</i>	Belcher and Elliott, 2001	2,700
371505116254501	<i>U-20WW</i>	Garcia and others, 2010	1,200
371434116251601	<i>U-20a-2WW</i>	Graves, 2002a	2,400
371353116282501	<i>U-20c</i>	Belcher and Elliott, 2001	1
371807116243001	<i>U-20g</i>	Belcher and Elliott, 2001	1
371744116272101	<i>U-20i</i>	Belcher and Elliott, 2001	1
370806116264001	<i>UE-18r</i>	Belcher and Elliott, 2001	3,100
371852116175701	<i>UE-19b-1</i>	Belcher and Elliott, 2001	7,500
371608116191002	<i>UE-19c</i>	Belcher and Elliott, 2001	1,600
371750116195901	<i>UE-19e</i>	Belcher and Elliott, 2001	1,100
371329116220302	<i>UE-19fS</i>	Graves, 2002b	1,000
371830116215300	<i>UE-19gS</i>	Graves, 2002c	2,500
372034116222501	<i>UE-19h</i>	Belcher and Elliott, 2001	19,000
371459116204812	<i>UE-19i</i>	Graves, 2002d	160
371442116243301	<i>UE-20bh1</i>	Belcher and Elliott, 2001	3,400
371452116284901	<i>UE-20d</i>	Belcher and Elliott, 2001	5,900
371901116272501	<i>UE-20e-1</i>	Belcher and Elliott, 2001	1,100
371617116291701	<i>UE-20f</i>	Graves, 2002e	30
371618116260201	<i>UE-20h</i>	Belcher and Elliott, 2001	1,400
371801116320301	<i>UE-20j</i>	Belcher and Elliott, 2001	7,900
372024116312001	<i>UE-20p</i>	Belcher and Elliott, 2001	1
370956116172101	<i>WW-8</i>	Belcher and Elliott, 2001	11,000

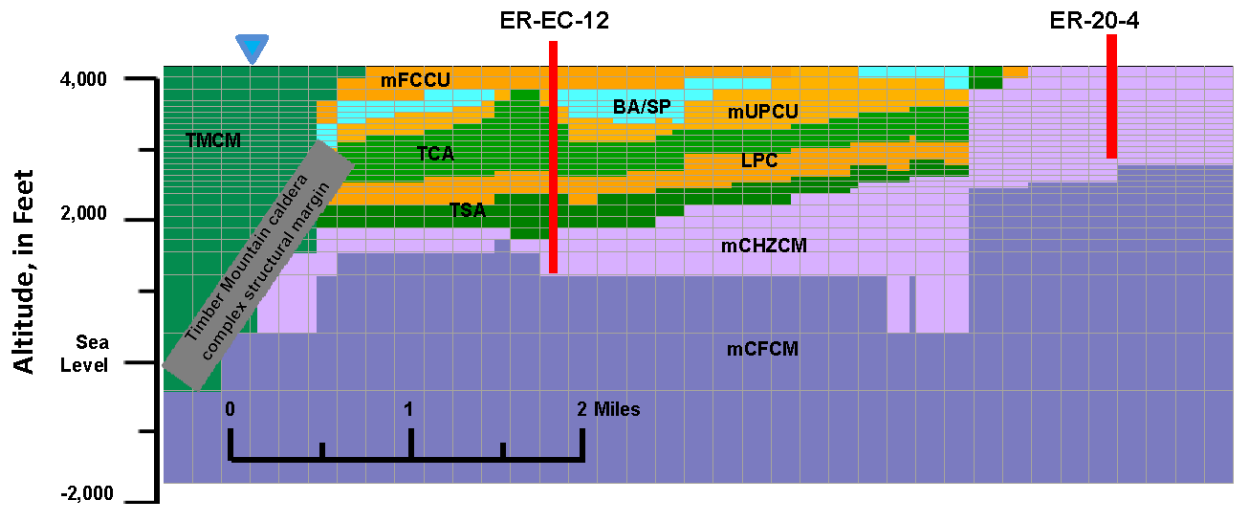


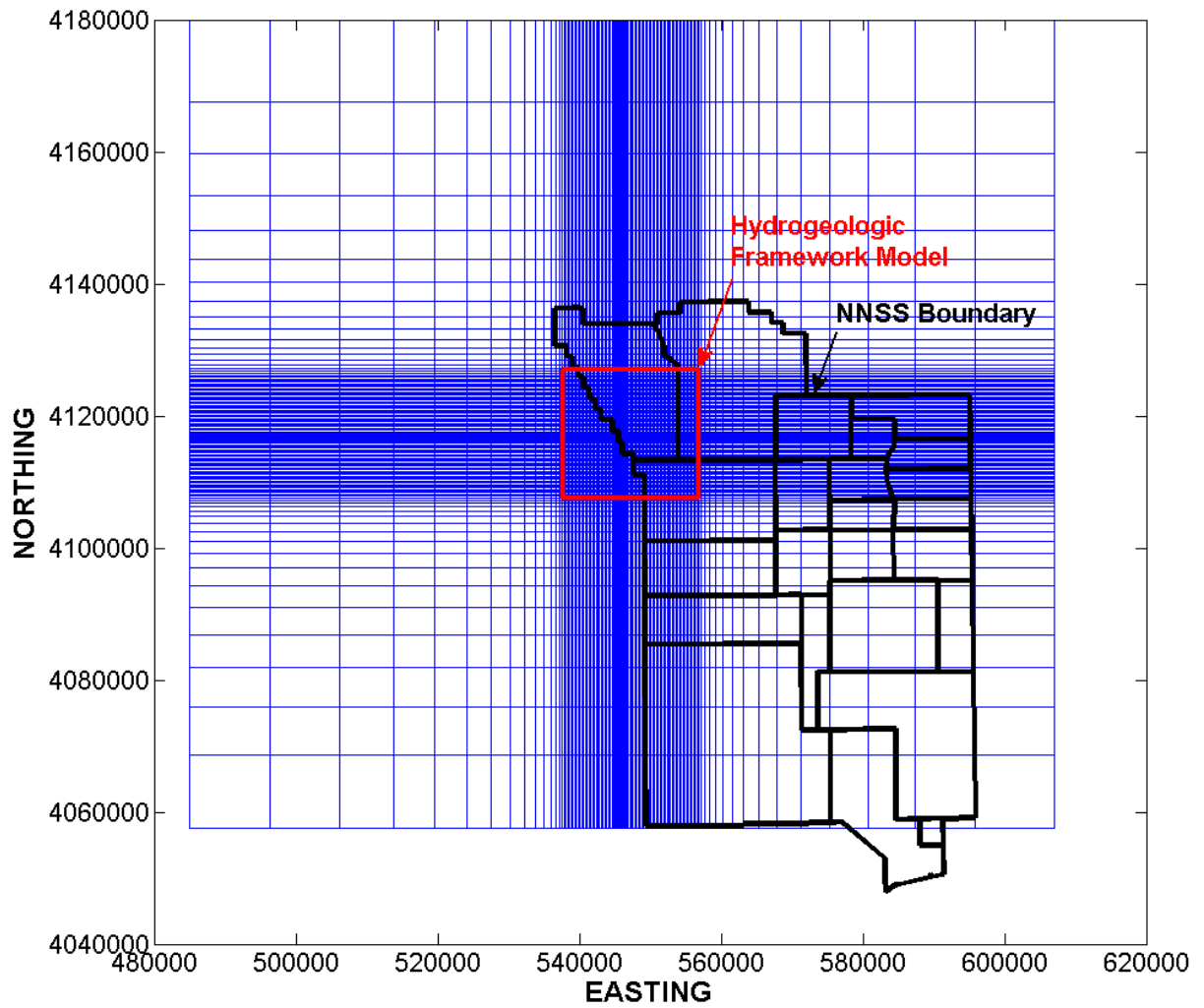
Figure 5. Cross-section showing vertical discretization and modified hydrostratigraphic units near the *ER-EC-12 main (upper and lower zone)* numerical groundwater-flow model.

Groundwater-Flow Models

Drawdowns from each multiple-well aquifer test were interpreted with three-dimensional MODFLOW models (Harbaugh and others, 2000). Each model was centered on the pumping well and each model grid extended laterally about 200,000 ft (38 mi) from the pumping well. All models were about 5,900 ft thick and extended vertically from 1,700 ft below sea level to 4,200 ft above sea level, which is the approximate water table (Figure 5). Rows and columns in the grid were assigned widths of 100 ft at the pumped well. Row and column widths increased successively by a factor of 1.25 away from the pumped well until groundwater-flow model cell widths equaled hydrogeologic framework cell widths of 820 ft. Row and column widths were a constant 820 ft until the hydrogeologic framework model edge was reached (delineated by red box in Figure 6). Row and column widths increased successively by a factor of 1.25 away from the hydrogeologic framework edge (red box in Figure 6) to the groundwater-flow model edge at a lateral distance of about 160,000 ft (30 mi). The number of rows and columns in each model was relatively consistent, with 113 to 114 rows and 115 to 116 columns (Table 5). All external boundaries were specified no-flow boundaries. Changes in the saturated thickness of the aquifer system were not simulated because the maximum drawdown near the water table was small relative to the total thickness. Variable discharge rates during each aquifer test were simulated with multiple stress periods, which were determined from simplified pumping schedules for each pumping well (Table 5).

A common vertical discretization was used in all groundwater-flow models to avoid structural inconsistencies and their potential effects on hydraulic property estimates. Discretization of groundwater-flow model layers was finer between 2,300 and 3,700 ft above sea level (Figure 5) where most pumped intervals occur. Groundwater-flow model layers gradually thickened from 2,300 ft above sea level to the base of the models where vertical discretization was relatively coarse.

All groundwater-flow models were discretized vertically into 29 layers. The top elevation of layer 1 defined the water table and the bottom elevation of layer 29 was equivalent to the elevation at the base of the hydrogeologic framework model (Figure 5). Layer 1 was 1-foot thick to better approximate drainage from the water table. Groundwater-flow model layers 2 to 4 were each 164-ft thick. Groundwater-flow model layers 5 to 20 were each 82-ft thick to capture thin HSUs, such as the mUPCU and LPCU in the vicinity of borehole *ER-EC-11*. Some modified HSUs such as the TCA and mCHZCM occur in multiple groundwater-flow model layers (Figure 5). Other modified HSUs such as the BA/SPA are locally absent in different parts of the groundwater-flow and hydrogeologic framework models.



Latitude and longitude coordinates are UTM zone 11, in meters.

Figure 6. Groundwater-flow model grid for the *ER-20-11* aquifer test.

Table 5. Pumping wells and number of layers, rows, columns and stress periods included in each groundwater-flow model.

Groundwater- Flow Model	Pumping Wells	Layers	Rows	Columns	Stress Periods
ER-20-4m	<i>ER-20-4 main</i>	29	113	115	6
ER-20-7	<i>ER-20-7</i>	29	114	116	6
ER-20-8m	<i>ER-20-8 main upper</i> <i>ER-20-8 main lower</i>	29	113	116	12
ER-20-8#2m	<i>ER-20-8 #2 main</i>	29	113	115	9
ER-20-11	<i>ER-20-11</i>	29	113	115	8
ER-EC-11m	<i>ER-EC-11 main</i>	29	114	115	6
ER-EC-12m	<i>ER-EC-12 main upper</i> <i>ER-EC-12 main lower</i>	29	113	115	8
ER-EC-13mUZ	<i>ER-EC-13 main upper</i>	29	113	116	10
ER-EC-13mLZ	<i>ER-EC-13 main lower</i>	29	113	116	8
ER-EC-14m	<i>ER-EC-14 main upper</i> <i>ER-EC-14 main lower</i>	29	113	116	10
ER-EC-15m	<i>ER-EC-15 main upper</i> <i>ER-EC-15 main intermediate</i> <i>ER-EC-15 main lower</i>	29	113	115	11

Parameter Estimation

Hydraulic conductivity, specific yield, and specific storage distributions were estimated by minimizing a weighted composite, sum-of-squares objective function. These distributions were defined with 1,768 pilot points where 1,250 pilot points were adjusted using Parameter ESTimation routine (PEST) (Doherty, 2008a). About 60 percent of adjustable pilot points defined the specific storage and specific yield distributions. Differences between measured and simulated observations defined the goodness-of-fit or improvement of calibration. These differences, or residuals, were weighted and summed in the objective function,

$$\Phi(x) = \sum_{i=1}^{nobs} [(\hat{o}_i - o_i)w_i]^2$$

where

- x is the vector of parameters being estimated,
- $nobs$ is the number of observations that are compared,
- (\hat{o}_i) is the i^{th} simulated observation,
- (o_i) is the i^{th} measurement or regularization observation, and
- w_i is the i^{th} weight.

Although the sum-of-squares error serves as the objective function, root-mean-square (RMS) error was reported because RMS error was compared easily to measurements. Root-mean-square error is,

$$RMS = \sqrt{\Phi / \sum_{i=1}^{nobs} w_i^2}$$

Measurement and regularization observations controlled model calibration. The models used 68,834 drawdowns as measurement observations (Table 6). Regularization observations guided hydraulic conductivity and specific yield estimates toward preferred conditions within similar HSUs and in areas that were insensitive to measurement observations. This approach is Tikhonov regularization (Doherty, 2008a).

The number of drawdown measurement observations was reduced by averaging drawdowns from each well to 6-hour intervals. Averaging reduced the number of measurement observations from more than 870,000 to 68,834 (Table 6) and suppressed high-frequency noise. Reliable observations were assigned weights greater than or equal to 0.5 (Table 6). Reliable drawdowns were defined as drawdowns not affected by pumping head losses, heating effects, wellbore storage, abridged records, or leaking bridge plugs (e.g., leakage across a bridge plug used to isolate multiple completion zones, resulting in drawdown responses from pumping upper and lower zones in a pumping well). Reliable observations totaled about 48,000 and were observed in 145 of 204 pumping-observation well pairs. Reliable observation weights were reduced to values between 0.5 and 1 at distant well clusters where similar

drawdown responses were observed in multiple wells so that model calibration would not be skewed toward these well clusters. For example, drawdown responses in wells *ER-EC-6 shallow*, *ER-EC-6 intermediate*, and *ER-EC-6 deep* to the *ER-EC-11 main* aquifer test were similar, and therefore were assigned weights of 0.5 to reduce sensitivity to these observations when calibrating the ER-EC-11m groundwater-flow model.

Drawdowns in a number of observation wells directly adjacent to and monitoring the pumped intervals were uncertain because the pumping well cluster was affected by head losses, heating effects, packer leakage, or wellbore storage. Measured drawdowns in well *ER-20-8 #2 main* during the *ER-20-8 #2 main* aquifer test were uncertain because of the strong correlation between pumping well head losses and aquifer response. Measured drawdowns in wells *ER-EC-11 main* and *ER-EC-11 upper intermediate* during the *ER-EC-11 main* aquifer test were very uncertain because of pumping head losses and heating effects. Measured drawdowns in observation wells *ER-EC-13 shallow*, *ER-EC-13 intermediate*, and *ER-EC-13 deep* during the *ER-EC-13 main upper and lower zone* aquifer tests were uncertain because of packer leakage. Measured drawdowns in observation wells *ER-EC-15 shallow*, *ER-EC-15 intermediate*, and *ER-EC-15 deep* during the *ER-EC-15 main upper zone* aquifer test were uncertain because of entry losses to the well and wellbore storage. In the above cases, measured drawdowns in observation wells in the annulus of the pumping well that were not adjacent to the pumped intervals were uncertain because of the effects of heating and leakage across bridge plugs.

Compromised observations in wells that were affected by head losses, heating effects, packer leakage, or wellbore storage in the pumping well cluster were assigned small weights (between 0.0001 and 0.1) so that hydraulic conductivity estimates were minimally affected. These effects were not simulated and can be significant where drawdowns exceed 100 ft and transmissivity of the pumped interval is less than 1,000 ft²/d. Parameter sensitivity also is proportional to the magnitude of simulated drawdowns, which can skew calibration toward fitting less certain measurements that are simulated poorly. Weights between 0.0001 and 0.01 were assigned to these observations because of measurement uncertainty, simulation inadequacy, and sensitivity adjustment. Measured drawdowns in observation wells in the annulus of the pumping well, which were not adjacent to the pumped intervals, but were affected by heating and leakage across bridge plugs, were assigned weights between 0.01 and 0.1 to reflect the uncertainty associated with these observations. Effects of weighting are reported with un-weighted and weighted sum-of-squares errors for each hydrograph ([Appendix B](#)).

Table 6. Pumping wells and number of observation wells and drawdown observations included in each groundwater-flow model.

Groundwater-Flow Model	Pumping Wells	Number of Observation Wells	Number of Observations		
			Original	6-Hour Average Drawdown	Weight Greater or Equal to 0.5
ER-20-4m	<i>ER-20-4 main</i>	6	18,492	1,480	1,072
ER-20-7	<i>ER-20-7</i>	14	65,098	1,076	936
ER-20-8m	<i>ER-20-8 main upper</i> <i>ER-20-8 main lower</i>	27	125,488	13,308	7,848
ER-20-8#2m	<i>ER-20-8 #2 main</i>	14	11,744	2,013	1,968
ER-20-11	<i>ER-20-11</i>	28	124,918	12,444	9,149
ER-EC-11m	<i>ER-EC-11 main</i>	13	8,683	1,595	1,475
ER-EC-12m	<i>ER-EC-12 main upper</i> <i>ER-EC-12 main lower</i>	10	68,970	5,091	4,816
ER-EC-13mUZ	<i>ER-EC-13 main upper</i>	20	77,684	5,540	4,696
ER-EC-13mLZ	<i>ER-EC-13 main lower</i>	22	61,466	5,314	5,109
ER-EC-14m	<i>ER-EC-14 main upper</i> <i>ER-EC-14 main lower</i>	23	122,287	9,275	7,905
ER-EC-15m	<i>ER-EC-15 main upper</i> <i>ER-EC-15 main intermediate</i> <i>ER-EC-15 main lower</i>	27	186,901	11,698	3,336
Total		204	871,731	68,834	48,310

Tikhonov regularization limited hydraulic conductivity and specific storage estimates at pilot points to reasonable values (Doherty and Johnston, 2003) in the absence of observation data indicating otherwise. Sharp differences between nearby values in similar modified HSUs were penalized to ensure relatively continuous hydraulic conductivity, specific yield, and specific storage distributions.

Regularization observations were equations that defined preferred relations between hydraulic conductivity estimates, specific yield estimates, and specific storage estimates. Regularization observations affected calibration most where the models were insensitive to measurement observations. Using regularization observations to impose preferred states, such as homogeneity within HSUs, was preferable to assigning fixed hydraulic property values within HSUs. A homogeneity condition allows hydraulic conductivity, specific yield, and specific storage estimates to differ where dictated by measured drawdowns.

Homogeneity within modified HSUs was the primary preferred relation between pilot points that defined hydraulic conductivity and specific storage. All pilot points defined specific yield at the water table (layer 1) regardless of modified HSUs present, which minimized the variance between specific yield estimates. About 29,000 regularization observations constrained hydraulic conductivity, specific yield, and specific storage estimates with these preferred relations.

Unrealistic hydraulic conductivity, specific yield, and specific storage distributions were avoided by limiting the fit between measured and simulated observations (Fiene and others, 2009). Irreducible measurement and numerical model errors were specified with the expected measurement error, known as PHIMEAS in PEST (Doherty, 2008a), which is a weighted, sum-of-squares error. Water-level modeling results suggest that the expected measurement RMS error should be about 0.02 ft (Garcia and others, 2013), which equals a PHIMEAS of 21 ft². A PHIMEAS of 19 ft² was specified and measurement error was reduced to 20 ft².

Drawdown Estimates

Drawdown estimates and their classification (i.e., detected, ambiguous, not detected) are documented previously in nine supporting memoranda ([Table 1](#)). Drawdown was classified as detected based on the signal-to-noise ratio and correlation between the pumping signal and environmental fluctuations. The signal-to-noise ratio is defined as the ratio of maximum drawdown in a well during an aquifer test to the RMS error. Correlation between the pumping signal and environmental fluctuations becomes apparent where observed drawdown can be approximated by a linear trend during all or part of the period of analysis. Correlation typically is possible as hydraulic diffusivity decreases, distance between observation and pumping well increases, or recovery is truncated. Correlation is unlikely where sharply defined pumping signals (saw-tooth) exist or significant recovery has been observed. Drawdown was classified as detected where the signal-to-noise ratio was greater than 10 and recovery was observed. Drawdown was classified as ambiguous when the signal-to-noise ratio ranged between 5 and 10, or greater than 10 if there was correlation or recovery was not observed. Drawdown was classified as not detected when the signal-to-noise ratio was less than 5.

Differences between measured and simulated drawdowns in observation well *ER-EC-6 shallow*, as determined from 9 groundwater-flow models and 14 of the 16 aquifer tests, respectively, are shown in [Figure 7](#) to illustrate differences between detected, ambiguous, and not detected drawdowns. Drawdown estimates in well *ER-EC-6 shallow* were reported as 1) detected during 6 aquifer tests in *ER-20-7*, *ER-20-8 main upper and lower zones*, *ER-20-8 #2 main*, *ER-20-11*, and *ER-EC-11 main*; 2) not detected during 7 aquifer tests in *ER-EC-12 main upper and lower zones*, *ER-EC-14 main upper and lower zones*, and *ER-EC-15 main upper, intermediate, and lower zones*; and 3) ambiguous during the *ER-EC-13 main lower zone* aquifer test. Drawdown was not estimated in well *ER-EC-6 shallow* during the *ER-20-4 main* aquifer test because drawdown was not detected in *ER-20-8 deep*, which is 6,800 ft closer to *ER-20-4 main* than *ER-EC-6 shallow*. Drawdown also was not estimated in well *ER-EC-6 shallow* during the *ER-EC-13 main upper zone* aquifer test because water-level data were corrupted (Damar and others, 2013a).

Drawdowns were detected at distances of up to 5 mi from pumping wells. The maximum distance where drawdown was detected occurred between pumping and observation well pair *ER-EC-14 main* and *ER-EC-1*, respectively (distance of 4.8 mi). Detected drawdowns in observation wells not located in the annulus of the pumping well ranged from 0.05 to 0.95 ft ([Appendix B](#)).

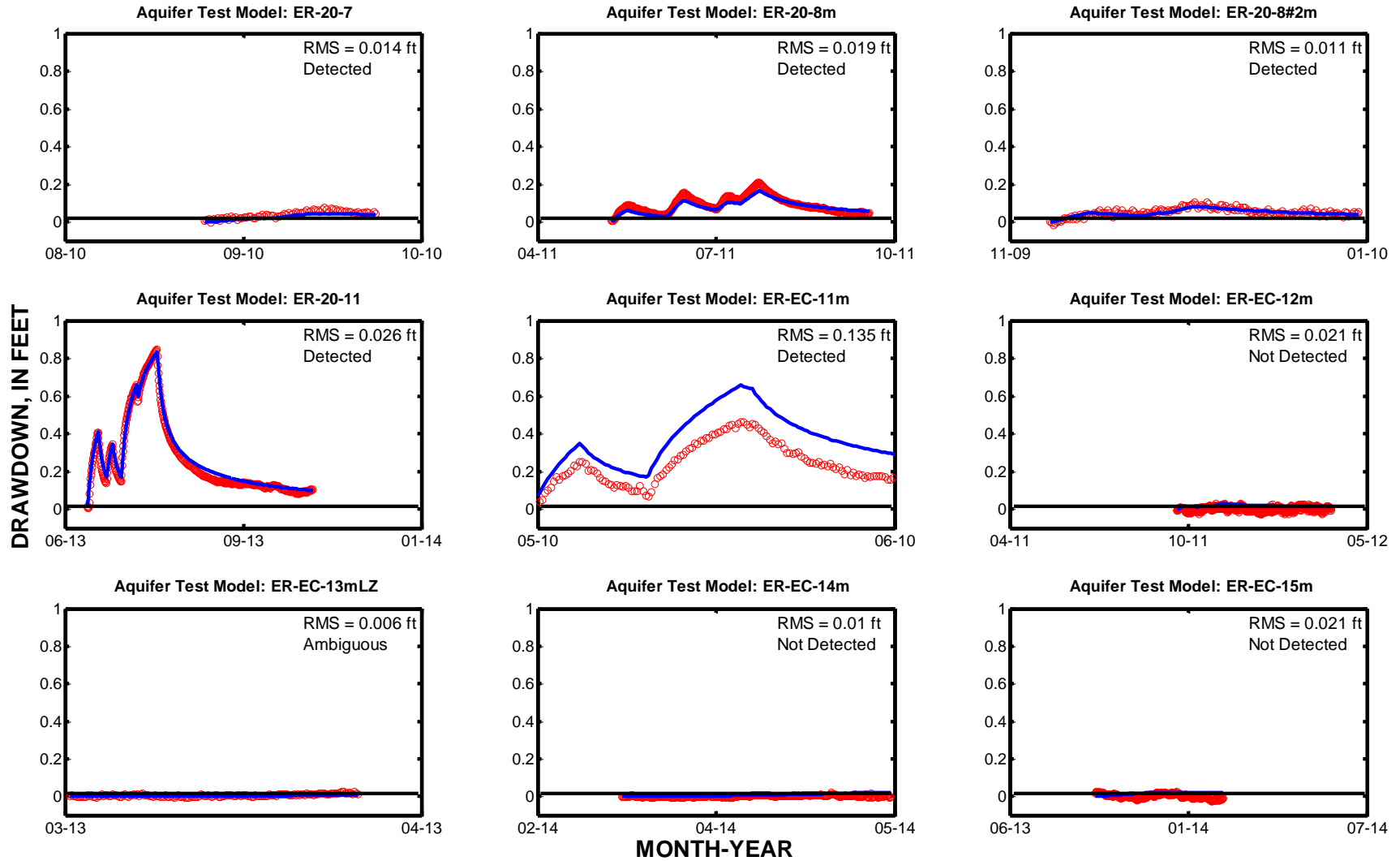


Figure 7. Simulated (BLUE) and estimated (RED) drawdowns in well *ER-EC-6 shallow* as determined from 9 groundwater-flow models and 14 aquifer tests.

Area Investigated

Areal extent and volume of investigation were defined using maximum simulated drawdown, which is the maximum simulated drawdown at a given location within the model domain from any of the 16 multiple-well aquifer tests. For example, the hydraulic head lowered a maximum of 0.91 ft in well *ER-EC-6 shallow* (Figure 7) during the 20th day of the *ER-20-11 main* aquifer test, and corresponds to the maximum simulated drawdown at this well site. A maximum simulated drawdown threshold of 0.05 ft was the criterion used for detecting simulated drawdown, which was supported by residual errors from water-level modeling to estimate drawdowns (Garcia et al., 2013). The extent of investigation where the maximum simulated drawdown exceeds a 0.05 ft drawdown threshold is a two-dimensional area that was defined by the maximum simulated drawdown at any depth (Figure 8). A total area of 60 mi² was investigated where maximum simulated drawdowns exceeded 0.05 ft (Figure 8). The widest areal extent of the 0.05 ft contour ranged from 9.5 to 10.3 mi.

Thirty-two of the thirty-four observation wells analyzed are located within the 0.05 ft drawdown area (Figure 8). These wells are predominantly located within the Bench area. Fewer observation wells (i.e., *ER-EC-2A*, *ER-EC-13*, and *ER-EC-14*) are located southwest of the Bench in the Timber Mountain moat structural domain and northeast of the NTMMSZ (i.e., *ER-20-1*, *ER-20-4*, *ER-20-5*, and *ER-20-7*) (Figure 8). Observation wells *ER-20-2-1* and *UE-18r* are located outside the 0.05 ft drawdown area. Well *ER-20-2-1* occurs within the mCHZCM north of the NTMMSZ and well *UE-18r* occurs within one of the Timber Mountain Composite Units south of the Bench.

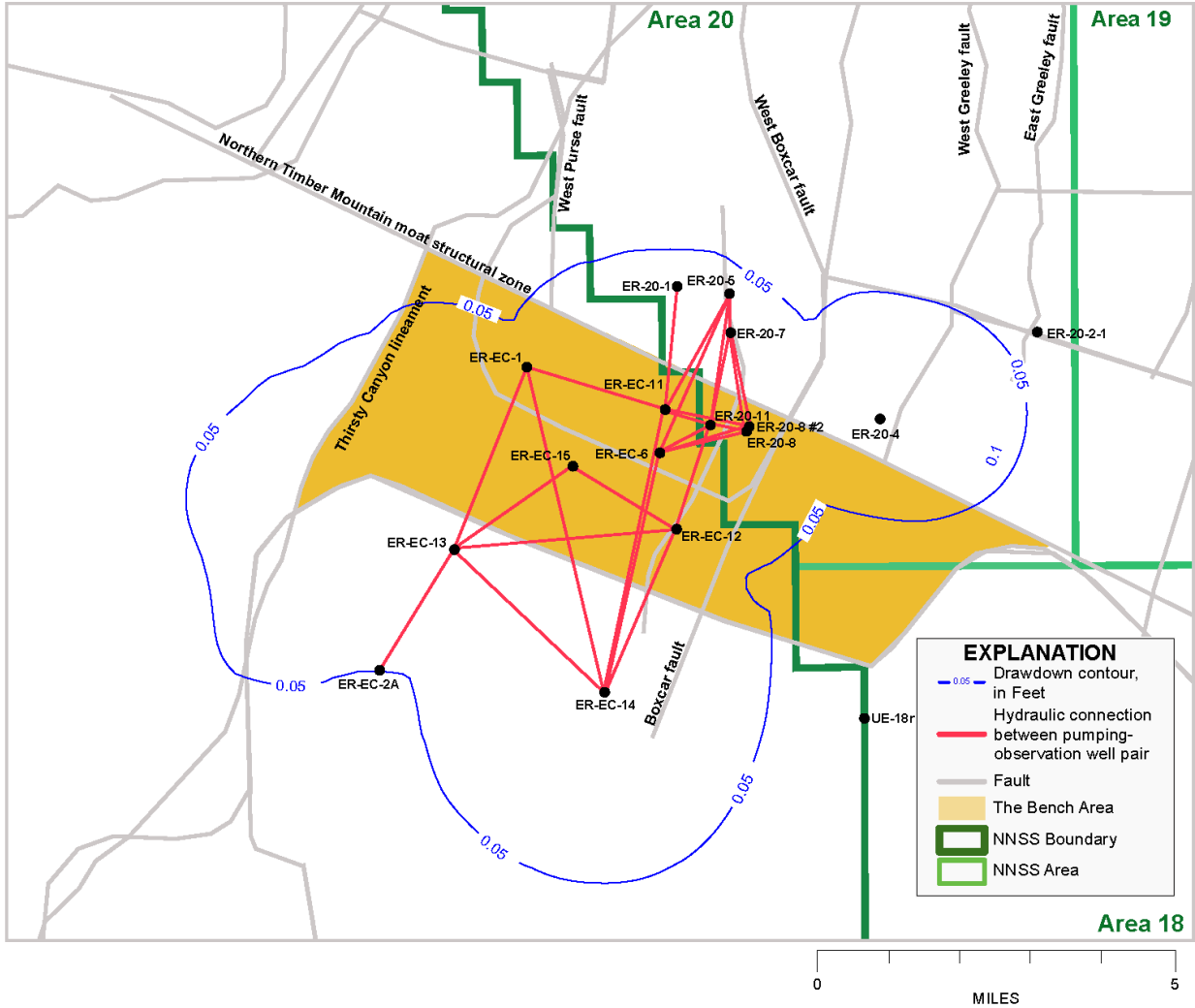


Figure 8. Maximum simulated drawdown that occurred at any time during one of the 16 aquifer tests and hydraulic connections between pumping-observation well pairs.

Hydraulic-Property Estimates

Transmissivity within modified HSUs around well sites was estimated from simultaneous analysis of groundwater-flow models. The spatial distribution of transmissivity estimates within the investigated area (≥ 0.05 ft of drawdown) is shown in [Figure 9](#). Total transmissivity ranged from 300 to 120,000 ft²/d in the investigated area.

Transmissivity estimates were highest near the northern and southern margins of the Bench ([Figure 9](#)). High transmissivity zones occur in the northeast part of the Bench near wells *ER-20-8*, *ER-20-8#2*, *ER-20-11*, and *ER-EC-11*, which are close to the NTMMSZ. High transmissivity zones also occur near the Timber Mountain caldera complex structural margin that borders the Bench to the south. At these margins, faulted and displaced rhyolitic lava flows, ash-flow tuffs, and welded-tuffs abut the margin of the Silent Canyon caldera complex to the north and the Timber Mountain caldera complex to the south. High transmissivity estimates could be attributed to enhanced permeability of disturbed zones near the contacts between two different structural features.

In general, estimated transmissivity for modified HSUs around well sites were greater within the Bench than within the caldera complexes to the north and south of the Bench ([Table 7](#)). Note that [Figure 9](#) shows transmissivity estimates were greater within the Timber Mountain caldera complex than within the Bench, whereas [Table 7](#) shows transmissivity estimates were greatest within the Bench. This anomaly occurs because transmissivity estimates in [Table 7](#) are computed by averaging transmissivity within a 300-ft radius around the wells. The BA/SPA, which comprises lava flows, is the most transmissive modified HSU, with a transmissivity estimate of 86,000 ft²/d around the *ER-20-8* well cluster. The mFCCU is the second-most transmissive modified HSU modeled around well sites, where the highest transmissivity estimate is 24,000 ft²/d around well *ER-20-11*. Transmissivity estimates for the mFCCU are uncertain because no pumping or observations wells are open to the unit. The Paintbrush Group is the most transmissive unit north of the Bench with a transmissivity estimate of 17,000 ft²/d around well *ER-20-7*. South of the Bench, transmissivity estimates are uncertain for the TMCM, which is a composite of welded-tuff aquifers and non-welded tuff confining units, largely because few wells penetrate the TMCM, and the area of investigation does not extend far into the Timber Mountain caldera complex. Transmissivity estimates within the TMCM and mCHZCM, located north of the Bench, were similar and ranged between 380 and 10,000 ft²/d.

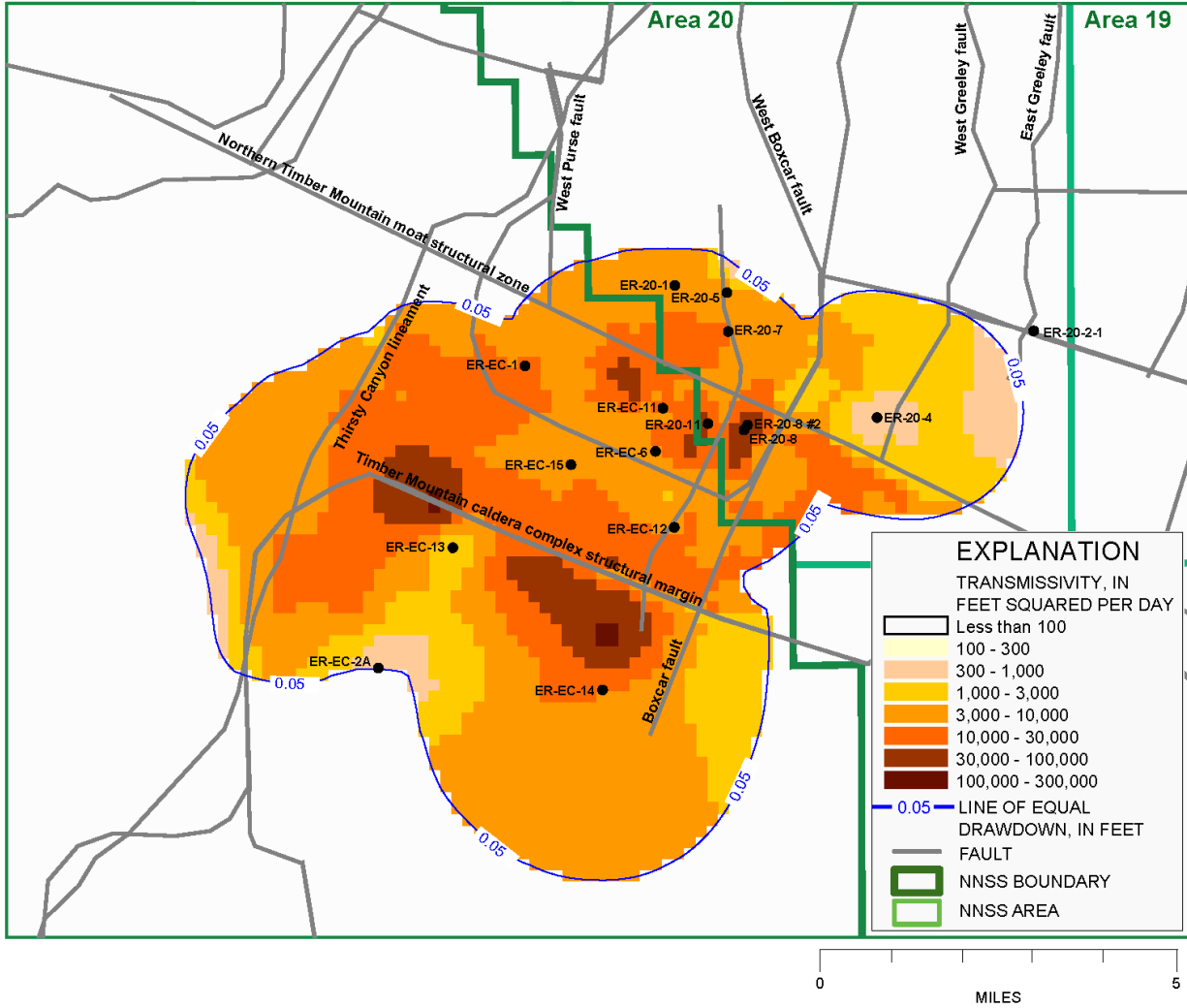


Figure 9. Transmissivity distribution within the investigated area where the maximum drawdown was equal to or exceeded 0.05 ft during simulation periods.

Table 7. Transmissivity estimates for modified hydrostratigraphic units surrounding observation and pumping well sites.

[All values are in feet squared per day; NA is Not Applicable; TMCM is the Timber Mountain composite unit; mFCCU includes the Tannenbaum Hill lava-flow aquifer (THLFA), Tannenbaum Hill composite unit (THCM), Timber Mountain aquifer (TMA), Fluorspar Canyon confining unit (FCCU), Windy Wash aquifer (WWA), and Paintbrush vitric-tuff aquifer (PVTA); BA/SPA is the Benham and Scrugham Peak aquifers; Paintbrush group includes the Upper Paintbrush confining unit (UPCU), Middle Paintbrush confining unit (MPCU), Tiva Canyon aquifer (TCA), lower Paintbrush confining unit (LPCU), and Topopah Spring aquifer (TSA); and mCHZCM includes the Calico Hills vitric composite unit (CHVCM), Calico Hills zeolitic composite unit (CHZCM), Calico Hills confining unit (CHCU), Belted Range aquifer (BRA), and Inlet aquifer (IA)]

Well	TMCM	mFCCU	BA/SPA	Paintbrush Group	mCHZCM	Total
ER-20-1	NA	NA	NA	2,200	3,800	6,000
ER-20-4 main	NA	NA	NA	NA	680	680
ER-20-5	NA	NA	NA	230	8,700	8,900
ER-20-7	NA	NA	NA	17,000	1,100	18,000
ER-20-8 main	NA	150	86,000	9,000	1,000	96,000
ER-20-8#2 main	NA	150	86,000	9,000	1,000	96,000
ER-20-11	NA	24,000	150	12,000	1,400	38,000
ER-EC-1	NA	860	6,300	4,000	680	12,000
ER-EC-2A	380	NA	NA	NA	NA	380
ER-EC-6	NA	3,800	6,300	1,500	400	12,000
ER-EC-11 main	NA	3,000	13,000	380	440	17,000
ER-EC-12 main	NA	3,300	4,200	29	440	8,000
ER-EC-13 main	1,400	NA	NA	NA	NA	1,400
ER-EC-14 main	9,800	NA	NA	NA	NA	9,800
ER-EC-15 main	NA	3,700	860	23	620	5,200

Transmissivity estimates around well sites (Figure 9) that are hydraulically connected to multiple pumping wells (Figure 8) are the most reliable. Transmissivity around well site *ER-EC-11 main* totaled 17,000 ft²/d (Table 7) and distributions among the HSUs likely are correct as drawdown at this well site was detected during 12 of the 16 aquifer tests (Table 7). More than 75 percent of the transmissivity at this well site is attributed to the BA/SPA. The dominance of transmissivity in the BA/SPA is consistent with higher concentrations of tritium that were measured in this HSU while drilling *ER-EC-11 main* (U.S. Department of Energy, 2012). Results shown here and from flow logs (Garcia and others, 2010) also indicate that most of the transmissivity at well sites *ER-EC-1*, *ER-EC-6*, and *ER-EC-12 main* occurs in the BA/SPA.

Specific yield and specific storage estimates averaged 0.02 and 3×10^{-6} 1/ft, respectively, for TMCM, mFCCU, BA/SPA, Paintbrush group, and mCHZCM units. About 50 percent of the specific yield estimates ranged between 0.01 and 0.05 and about 20 percent of the estimates exceeded the expected range between 0.001 and 0.05.

References Cited

- Bechtel Nevada, 2002, A hydrostratigraphic model and alternatives for the groundwater flow and contaminant transport model of Corrective Action Units 101 and 102— Central and western Pahute Mesa, Nye County, Nevada: U.S. Department of Energy Report DOE/NV/11718—706, 383 p.
- Belcher, W.R., and Elliott, P.E., 2001, Hydraulic-property estimates for use with a transient ground-water flow model of the Death Valley regional ground-water flow system, Nevada and California: U.S. Geological Survey Water-Resources Investigations Report 01-4210, 34 p.
- Damar, N., Reiner, S., and Halford, K.J., 2013a, Drawdown estimation in wells outside of the *ER-EC-13* well site during the *ER-EC-13 main upper zone* aquifer test, June 22–August 3, 2012, Pahute Mesa, Nevada National Security Site, (See Appendix D).
- Damar, N., Reiner, S., Halford, K.J., and Mirus, B.B., 2013b, Drawdown estimation in wells outside of the *ER-EC-13* well site during the *ER-EC-13 main lower zone* aquifer test, March 7–29, 2013, Pahute Mesa, Nevada National Security Site, (See Appendix D).
- Doherty, J., and J.M. Johnston, 2003, Methodologies for calibration and predictive analysis of a watershed model: *Journal of American Water Resources Association*, v. 39, no. 2, p. 251-265.
- Doherty, J., 2008a, *PEST: Model-Independent Parameter Estimation*. Brisbane, Australia: Watermark Numerical Computing.
- Doherty, J., 2008b, *PEST Groundwater Data Utilities*. Brisbane, Australia: Watermark Numerical Computing.
- Fenelon, J., Reiner, S., and Laczniak, R.J., 2009, *AQUIFER-TEST PACKAGE—Analysis of U-20 WW multiple-well aquifer test, Pahute Mesa, Nevada Test Site*: U.S. Geological Survey Aquifer-Test Package, available at 'Nevada Water Science Center Aquifer Tests' webpage, accessed August 18, 2014, at http://nevada.usgs.gov/water/aquifertests/nts_singlewell_U-20ww.cfm?studynome=nts_singlewell_U-20ww
- Fienen, M., Muffels, C., and Hunt, R., 2009, On constraining pilot point calibration with regularization in PEST, *Ground Water*, v. 47, no.6, p. 835–844.

- Garcia, C.A., Halford, K.J., and Fenelon, J.M., 2013, Detecting drawdowns masked by environmental stresses using Theis transforms. *Ground Water*, 51(3), p. 322-332.
- Garcia, C.A., Halford, K.J., and Lacznia, R.J., 2010, Interpretation of flow logs from Nevada Test Site boreholes to estimate hydraulic conductivity using numerical simulations constrained by single-well aquifer tests: U.S. Geological Survey Scientific Investigations Report 2010–5004, 28 p.
- Garcia, C.A., Reiner, S., and Halford, K.J., 2012, Drawdown estimation for the *ER-20-8 main upper and lower zone* multiple-well aquifer test, Pahute Mesa, Nevada National Security Site, (See Appendix D).
- Garcia, C.A., Jackson, T.R., Reiner, S., and Halford, K.J., 2014, Drawdown estimation for the *ER-EC-14 main upper and lower zones* multiple-well aquifer tests, Pahute Mesa, Nevada National Security Site, (See Appendix D).
- Graves, R., 2002a, Aquifer-Test Report for Test Well U-20a-2: U.S. Geological Survey Aquifer-Test Package, available at ‘Nevada Water Science Center Aquifer Tests’ webpage, accessed August 18, 2014, at http://nevada.usgs.gov/water/aquifertests/nts_singlewell_U-20a-2.cfm?studyname=nts_singlewell_U-20a-2
- Graves, R., 2002b, Aquifer-Test Report for Test Well UE-19fS: U.S. Geological Survey Aquifer-Test Package, available at ‘Nevada Water Science Center Aquifer Tests’ webpage, accessed August 18, 2014, at http://nevada.usgs.gov/water/aquifertests/nts_singlewell_UE-19fs.cfm?studyname=nts_singlewell_UE-19fs
- Graves, R., 2002c, Aquifer-Test Report for Test Well UE-19gS: U.S. Geological Survey Aquifer-Test Package, available at ‘Nevada Water Science Center Aquifer Tests’ webpage, accessed August 18, 2014, at http://nevada.usgs.gov/water/aquifertests/nts_singlewell_UE19gs.cfm?studyname=nts_singlewell_UE19gs
- Graves, R., 2002d, Aquifer-Test Report for Test Well UE-19i: U.S. Geological Survey Aquifer-Test Package, available at ‘Nevada Water Science Center Aquifer Tests’ webpage, accessed August 18, 2014, at http://nevada.usgs.gov/water/aquifertests/nts_singlewell_UE-19i.cfm?studyname=nts_singlewell_UE-19i
- Graves, R., 2002e, Aquifer-Test Report for Test Well UE-20f: U.S. Geological Survey Aquifer-Test Package, available at ‘Nevada Water Science Center Aquifer Tests’ webpage, accessed August 18, 2014, at http://nevada.usgs.gov/water/aquifertests/nts_singlewell_UE-20f.cfm?studyname=nts_singlewell_UE-20f

- Halford, K.J., Fenelon, J.M., and Reiner, S.R., 2010, Analysis of ER-20-8 #2 and ER-EC-11 multiple-well aquifer tests, Pahute Mesa, Nevada National Security Site: U.S. Geological Survey Aquifer-Test Package, available at 'Nevada Water Science Center Aquifer Tests' webpage, accessed August 15, 2014, at http://nevada.usgs.gov/water/aquifertests/er_wells.cfm?studynome=er_wells
- Halford, K.J., Fenelon, J.M., and Reiner, S.R., 2011, Estimates of drawdowns from ER-20-7 and ER-20-8 main upper zone multiple-well aquifer tests and simultaneous numerical analysis of four recent aquifer tests to estimate hydraulic properties on Pahute Mesa, Nevada National Security Site: U.S. Geological Survey Aquifer-Test Package, available at 'Nevada Water Science Center Aquifer Tests' webpage, accessed August 15, 2014, at http://nevada.usgs.gov/water/aquifertests/er_wells_mainupperzone.cfm?studynome=er_wells_mainupperzone
- Halford, K.J., Fenelon, J.M., and Reiner, S.R., 2012, Simultaneous numerical analysis of eight aquifer tests to estimate hydraulic properties on Pahute Mesa, Nevada National Security Site: U.S. Geological Survey Aquifer-Test Package, available at 'Nevada Water Science Center Aquifer Tests' webpage, accessed August 15, 2014, at http://nevada.usgs.gov/water/AquiferTests/Pahute_Mesa_8.cfm?studynome=Pahute_Mesa_8
- Halford, Keith J., C. Amanda Garcia, and Steve Reiner, 2012, AQUIFER TEST--Analysis of ER-20-4 main, single-well aquifer test of volcanic rocks, Pahute Mesa, Nevada National Security Site: U.S. Geological Survey Aquifer-Test Package, available at 'Nevada Water Science Center Aquifer Tests' webpage, accessed September 8, 2014, at <http://nevada.usgs.gov/water/AquiferTests/ER-20-4.cfm?studynome=ER-20-4>
- Halford, Keith J. and Steve Reiner, 2012, AQUIFER TEST--Analysis of ER-EC-12 main lower, single-well slug test of volcanic rocks, Pahute Mesa, Nevada National Security Site: U.S. Geological Survey Aquifer-Test Package, available at 'Nevada Water Science Center Aquifer Tests' webpage, accessed September 8, 2014, at <http://nevada.usgs.gov/water/AquiferTests/ER-EC-12ML.cfm?studynome=ER-EC-12ML>
- Halford, Keith J. and Steve Reiner, 2013, AQUIFER TEST-- Analysis of *ER-EC-13 main upper zone* and *ER-EC-13 main lower zone*, multiple-well aquifer test of volcanic rocks, Pahute Mesa, Nevada National Security Site: U.S. Geological Survey Aquifer-Test Package, available at 'Nevada Water Science Center Aquifer Tests' webpage, accessed September 8, 2014, at http://nevada.usgs.gov/water/AquiferTests/ER-EC-13_MUZ_MLZ.cfm?studynome=ER-EC_13_MUZ_MLZ

- Halford, Keith J. and Steve Reiner, 2014, AQUIFER TESTS—Analyses of *ER-EC-15 main upper zone*, *ER-EC-15 main intermediate zone*, and *ER-EC-15 main lower zone*, single-well aquifer tests of volcanic rocks, Pahute Mesa, Nevada National Security Site, September 2014, (See Appendix D).
- Harbaugh, A.W., Banta, E.R., Hill, M.C., and McDonald, M.G., 2000, MODFLOW- 2000, the U.S. Geological Survey modular ground-water model -- User guide to modularization concepts and the Ground-Water Flow Process: U.S. Geological Survey Open-File Report 00-92, 121 p.
- Jackson, Tracie R. and Keith Halford, 2014, Drawdown estimation for *ER-20-11*, Pahute Mesa, Nevada National Security Site, May 2014, (See Appendix D).
- Laczniak, R.J., Cole, J.C., Sawyer, D.A., and Trudeau, D.A., 1996, Summary of hydrogeologic controls on ground-water flow at the Nevada Test Site: U.S. Geological Survey Water-Resources Investigations Report 96-4109, 59 p.
- Mirus, Benjamin, C. Amanda Garcia, Steve Reiner, and Keith Halford, 2012a, Drawdown estimation for the *ER-20-4* multiple-well aquifer test, Pahute Mesa, Nevada National Security Site, July-2012, (See Appendix D).
- Mirus, Benjamin, C. Amanda Garcia, Steve Reiner, and Keith Halford, 2012b, Drawdown estimation for the *ER-EC-12 main upper and lower zone* multiple-well aquifer test, Pahute Mesa, Nevada National Security Site, (See Appendix D).
- Oberlander, P.L, Lyles, B.F., and Russell, C.E., 2002, Summary report, Borehole testing and characterization of western Pahute Mesa - Oasis Valley ER-EC wells: Desert Research Institute Publication 45195, 56 p.
- Oberlander, P.L, McGraw, D., and Russell, C.E., 2007, Final report, Hydraulic conductivity with depth for Underground Test Area (UGTA) wells: Desert Research Institute Publication 45228, 237 p.
- Prothro, L.B. and Drellack, S.L., Jr., 1997, Nature and extent of lava-flow aquifers beneath Pahute Mesa, Nevada Test Site: U.S. Department of Energy Report DOE/NV/11718-156, 50 p.
- RamaRao, B.S., de Marsily, G., and Marietta, M.G., 1995, Pilot point methodology for automated calibration of an ensemble of conditionally simulated transmissivity fields 1. Theory and computational experiments: *Water Resources Research*, v. 31, no. 3, p. 475–493.
- Theis, C.V., 1935, The relation between the lowering of the piezometric surface and the rate and duration of discharge of a well using groundwater storage: *Am. Geophys. Union Trans.*, vol. 16, pp. 519-524.

- U.S. Department of Energy, 1997, Completion report for well cluster ER-20-5: U.S. Department of Energy Report DOE/NV-466/UC-700.
- U.S. Department of Energy, 2000, Completion report for well cluster ER-EC-6: U.S. Department of Energy Report DOE/NV/11718-360.
- U.S. Department of Energy, 2002a, Completion report for well ER-EC-2A: U.S. Department of Energy Report DOE/NV/11718-591.
- U.S. Department of Energy, 2002b, Analysis of Well ER-18-2 testing, western Pahute Mesa—Oasis Valley FY 2000 Testing Program: U.S. Department of Energy Report DOE/NV/13052—845.
- U.S. Department of Energy, 2002c, Analysis of well ER-EC-8 testing, western Pahute Mesa—Oasis Valley FY 2000 Testing Program: U.S. Department of Energy Report DOE/NV/13052—179.
- U.S. Department of Energy, 2009, Phase II corrective action investigation plan for Corrective Action Units 101 and 102--Central and western Pahute Mesa, Nevada Test Site, Nye County, Nevada: U.S. Department of Energy Report DOE/NV--1312, Rev. 2, 255 p.
- U.S. Department of Energy, 2010a, Completion report for well ER-20-7, Corrective Action Units 101 and 102: Central and Western Pahute Mesa: U.S. Department of Energy Report DOE/NV--1386.
- U.S. Department of Energy, 2010b, Completion report for well ER-EC-11, Corrective Action Units 101 and 102: Central and Western Pahute Mesa: U.S. Department of Energy Report DOE/NV--1435.
- U.S. Department of Energy, 2011a, Completion report for wells ER-EC-13, Corrective Action Units 101 and 102: Central and Western Pahute Mesa: U.S. Department of Energy Report DOE/NV--1448.
- U.S. Department of Energy, 2011b, Completion report for wells ER-EC-15, Corrective Action Units 101 and 102: Central and Western Pahute Mesa: U.S. Department of Energy Report DOE/NV--1449.
- U.S. Department of Energy, 2012, Pahute Mesa Well Development and Testing Analyses for Wells ER-20-8 and ER-20-4, Nevada National Security Site, Nye County, Nevada: U.S. Department of Energy Report DOE/NV—Preliminary, Revision No.: 0, August 2012.

U.S. Geological Survey, 2014, 'Nevada Water Science Center Aquifer Tests' webpage, accessed September 8, 2014, at <http://nevada.usgs.gov/water/aquifertests/index.htm>

Appendix A

Appendix A shows the construction of pumping and observation wells monitored during aquifer testing at Pahute Mesa as well as hydrostratigraphic units penetrated by wells.

Appendix B

All water level data from pumping and observation wells during the following 16 aquifer tests are in the zipped file, AppendixB: *ER-20-4 main, ER-20-7, ER-20-8 main upper and lower zones, ER-20-8 #2, ER-20-11, ER-EC-11 main, ER-EC-12 main upper and lower zones, ER-EC-13 main upper and lower zones, ER-EC-14 main upper and lower zones, and ER-EC-15 upper, intermediate, and lower zones*. The zip file contains figures in GIF format. Figures show time series of 6-hour averaged measured drawdown, simulated drawdown, raw drawdown from water-level models, and simplified pumping schedules. For each figure, the following statistics are reported: unweighted sum-of-squares error, weighted sum-of-squares error, and root-mean-square error.

Appendix C

The 11 MODFLOW groundwater-flow models used to simulate pumping and recovery responses during the 16 aquifer tests are in the zipped file, AppendixC. The zip file contains: (1) an Exec directory comprised of FORTRAN executables for running MODFLOW and PEST applications; (2) a MASTER directory comprised of PEST output files and a universal set of hydraulic parameters for all groundwater-flow models; and (3) eleven subfolders for the eleven groundwater-flow models which comprise MODFLOW input and output files. To run all groundwater-flow models using the MODFLOW executable, go to the MASTER directory and double-click batch file: 01_MF_ALL.bat. To obtain PEST statistics for all groundwater-flow models at the zeroth iteration (best solution parameters), go to the MASTER directory and double-click batch file: 00_PEST_PM.bat. PEST output files are written to the MASTER directory. To run a single groundwater-flow model, go to the directory of the MODFLOW model, denoted by the prefix 'MF_' for each aquifer test model, and double-click batch file: 01_MF_Build-Call-Extract.bat.

Appendix D

Unpublished drawdown and aquifer test reports are in AppendixD.zip file.